

## Aspects of CompHEP applications to hadronic collider physics

---

**M.N. Dubinin\***

*Skobeltsyn Institute of Nuclear Physics, Moscow State University*

*Leninskiye Gory, 119991 Moscow, Russian Federation*

*E-mail: dubinin@theory.sinp.msu.ru*

Various technical aspects of CompHEP version 4.5 applications to the Tevatron and the LHC physics analyses and unweighted event generation are reviewed. Using the channel  $pp \rightarrow \gamma\gamma + 2 \text{ jets}$  (irreducible background to Higgs boson production by vector boson fusion at the LHC) as an example, we describe the fine tuning of the numerical interface in CompHEP, the efficiency of simplification of flavor combinatorics, the need for parallel processing and mention briefly other recent developments.

*CPP 2010 - 3rd Computational Particle Physics Workshop*

*23-25 September 2010*

*KEK, Tsukuba, Japan*

---

\*Speaker.

## 1. Introduction

More than twenty years passed since the general plan for the CompHEP project development [1] was proposed. The primary version of CompHEP used the Pascal language for PC AT and generated automatically REDUCE [2] format code for the squared amplitude corresponding to a gauge-invariant set of diagrams [3]. It was expected that analytic results for differential and total cross sections could be obtained and then used to explain an experimental data. Obviously such strategy of development did not allow to reduce bulky symbolic expressions for complete sets of tree-level diagrams to an acceptable form, this motivated the development of FORTRAN code automatic generation modules amenable to the following Monte Carlo (MC) integration by means of BASES generator [4] which was provided by the GRACE [5] team. Jointly, although using different methods, MC calculations were performed for a large set of processes [6], which has allowed to test reliably all the algorithms involved. First phenomenological applications were related to  $\gamma e$  and  $\gamma\gamma$  modes of JLC and TESLA colliders [7], in the following the channels of four-fermion production at LEP2 were analysed at complete tree-level [8]. Numerous tests of CompHEP and GRACE algorithms and comparisons of results for a large set of physical channels were of prime importance for the following applications to leptonic and hadronic collider physics.

In latest years extensive generation of unweighted events and important analyses for Tevatron and LHC colliders have been performed by means of CompHEP version 4 [9]. Recently the single top quark production at the Tevatron  $p\bar{p}$  collider was simulated. CompHEP based calculations of complete tree-level sets of diagrams and the following event generation at the next-to-leading order (NLO) level were used for the first direct observation of a single top quark signal in D0 experiment [10]. Experimental detection of a single top quark is important for searches of new physics. Applications of CompHEP have been considered for the Higgs boson detection at the LHC in the framework of the CMS collaboration. The simulation of the Higgs boson signal at the LHC can be sensibly performed only for complete sets of tree-level diagrams, when the huge backgrounds, typical for hadronic colliders, can be put under control. Note than in addition to the irreducible background diagrams large contributions arise from the complete sets where jets are misidentified as photons, which also must be carefully simulated. A number of technical developments which had been implemented for the single top quark simulation and are going to be used in the LHC analyses are described in some details below.

## 2. Some aspects of simulation

The  $H \rightarrow \gamma\gamma$  decay is the most promising signal for the Higgs boson detection at the LHC in the mass region from 115 to 150 GeV [11]. Full CMS detector simulation [12] for the vector boson fusion (VBF) mode, where the photon pair is accompanied by two jets with large rapidity [13], should be done using large enough unweighted event samples of QCD jet background. The signal cross section is about 9 fb, while the QCD background is huge (of the order of  $10^9$  pb if no preselection cuts are applied). It is especially important to estimate directly the two photon misidentification background. Generator level (or partonic level) studies [14] which have been using estimates for the rate at which a jet would be misidentified as a photon do not account for any correlations within an event, use an oversimplified detector geometry when non-Gaussian tails in

the resolution are not adequately simulated, and are generally speaking unsatisfactory for careful analysis which is important in a complicated background environment of the hadronic collider.

In CompHEP calculation the backgrounds are defined on the level of complete tree-level diagram sets

- The irreducible QCD background  $\gamma\gamma+2$  jets from the 34 ( $u\#,d\#$ ) partonic subprocesses  $2 \rightarrow 4$  listed in Table 1. Main contribution comes from the subprocesses with  $u\#$ -quark and gluon in the initial state  $u\#g \rightarrow \gamma\gamma gu\#$  and  $gu\# \rightarrow \gamma\gamma gu\#$ . The amplitude of  $u\#g \rightarrow \gamma\gamma gu\#$  is given by the sum of 15 Feynman diagrams shown in Fig.1. Subleading contributions come from  $\bar{u}\#g \rightarrow \gamma\gamma g\bar{u}\#, g\bar{u}\# \rightarrow \gamma\gamma g\bar{u}\#, u\#u\# \rightarrow \gamma\gamma u\#u\#$  and  $gg \rightarrow \gamma\gamma u\#\bar{u}\#$ .
- The misidentification QCD background in the channel  $pp \rightarrow \gamma+3$  jets from 50 partonic subprocesses  $2 \rightarrow 4$  listed in Table 1. Main contribution comes from the subprocesses with  $u\#$ -quark and gluon in the initial state  $u\#g \rightarrow \gamma ggu\#$  and  $gu\# \rightarrow \gamma ggu\#$ .
- The irreducible and misidentification electroweak backgrounds. <sup>1</sup>

Unacceptably large number of partonic subprocesses is significantly reduced using the approximations of block-diagonal CKM matrix  $V_{CKM} = ((V,0)(0,1))$  and massless quarks of the first and the second generations [17] <sup>2</sup> Diagrams can be separated into gauge invariant classes with the scattering, exchange or annihilation topologies applying in the following a transportation of Cabibbo mixing from charged current vertices of the matrix element squared to the convolution of partonic distribution functions (PDF's). Trivial example of the simplification of quark combinatorics is given by the process of two jet production in the scattering of one up-quark and one down-quark, where 16 partonic subprocesses contribute: (1)  $ud \rightarrow ud, ud \rightarrow cd, ud \rightarrow us, ud \rightarrow cs$ ; (2)  $us \rightarrow us, us \rightarrow cs, us \rightarrow ud, us \rightarrow cd$ ; (3)  $cd \rightarrow cd, cd \rightarrow ud, cd \rightarrow cs, cd \rightarrow us$ ; (4)  $cs \rightarrow cs, cs \rightarrow us, cs \rightarrow cd, cs \rightarrow ud$ . If we denote the matrix element for the scattering (neutral current) topology by  $M_{sc}$  and the matrix element for the exchange (charged current) topology by  $M_{ex}$ , then the hadronic-level matrix element squared  $|M|^2$  can be rewritten in the form

$$(f_u + f_c)(f_d + f_s)(M_{sc}M_{sc}^* + M_{ex}M_{ex}^*) + 2(f_u f_d \cos^2 \theta_c + f_u f_s \sin^2 \theta_c + f_c f_d \sin^2 \theta_c + f_c f_s \cos^2 \theta_c)M_{sc}M_{ex}^*$$

where  $f_i(x, Q^2)$  are PDF's for the  $i$ -th quark specie and  $\theta_c$  is Cabibbo mixing angle. Such structure of  $|M|^2$  is automatically generated by CompHEP in the schemes `_SM_ud` and `_SM_qQ` from the list of build-in models. Corresponding input of the process string is  $u\#d\# \rightarrow u\#d\#$  where the 'hash' symbol specifies up- and down-quarks as subjects of the abovementioned simplifying procedures.

Cross sections in Table 1 for the irreducible background are calculated at the  $p_T \geq 20$  GeV for photons and jets and the separation  $\Delta R_{ij} \geq 0.4$ . For the reducible background additional preselection of two jets in the opposite hemispheres with the rapidity gap greater then 3.5 is introduced. CompHEP package evaluates precisely the squared amplitudes for all 34/50 partonic subprocesses

<sup>1</sup>Important sources which were carefully calculated, however, details are not described here. The cross section for the irreducible electroweak background (20 partonic subprocesses) is only 0.33 fb, but the event topology is very similar to the signal.

<sup>2</sup>In the case under consideration 4404 diagrams in 260 subprocesses (when the two quark generations are accounted for) are reduced to only 618 diagrams in 34 subprocesses.

of the irreducible/misidentification backgrounds by means of adaptive Monte-Carlo integration and then generates unweighted events at the partonic level with the following shower evolution and hadronization interfaced to PYTHIA [15]. For example, diagrams of the leading QCD partonic subprocess  $ug \rightarrow \gamma\gamma gu$  of the irreducible background are shown in Fig.1.

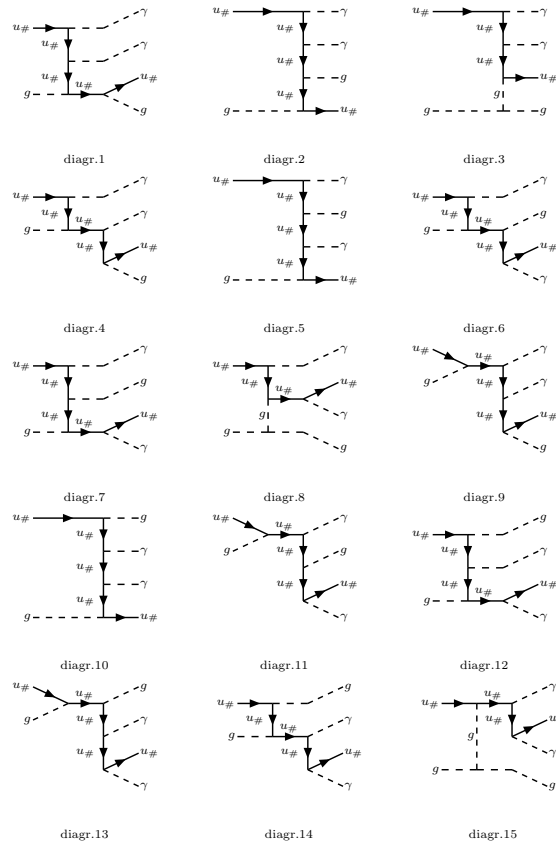


**Figure 1:** Complete set of  $2 \rightarrow 4$  tree level diagrams for the partonic subprocess No.7 (see the list of subprocesses in Table 1)  $u\#g \rightarrow \gamma\gamma u\#g$ .

Note that no any effective approximations are used in the event generation by CompHEP. The event generators which are using built-in software libraries for  $2 \rightarrow 2$  matrix elements 'upgrade' them to the level of  $2 \rightarrow 4$  in the framework of the scheme

$$\begin{aligned}
A_{34} = & I_g^u \otimes I_u^g \otimes A_{10}(u\bar{u} \rightarrow \gamma\gamma) + I_\gamma^u \otimes I_u^g \otimes [A_2(u\bar{u} \rightarrow \gamma g) + A_5(u\bar{u} \rightarrow \gamma g)] \\
& + [A_4(ug \rightarrow u\gamma) + A_6(ug \rightarrow u\gamma) + A_9(ug \rightarrow u\gamma) + A_{11}(ug \rightarrow u\gamma)] \otimes F_\gamma^u \otimes F_g^u \\
& + I_\gamma^u \otimes A_1(ug \rightarrow u\gamma) \otimes F_g^u + I_g^u \otimes A_{12}(ug \rightarrow u\gamma) \otimes F_\gamma^u \\
& + I_g^g \otimes [A_8(ug \rightarrow u\gamma) + A_{15}(ug \rightarrow u\gamma)] \otimes F_\gamma^u + I_\gamma^u \otimes I_g^g \otimes A_3(ug \rightarrow u\gamma) \\
& + I_\gamma^u \otimes A_7(ug \rightarrow ug) \otimes F_\gamma^u + [A_{13}(ug \rightarrow ug) + A_{14}(ug \rightarrow ug)] \otimes F_\gamma^u \otimes F_\gamma^u
\end{aligned}$$

where, for example,  $I_g^u \otimes I_u^g \otimes A_{10}(u\bar{u} \rightarrow \gamma\gamma)$  denotes the ladder diagram No.10 in Fig.1 evaluated as the convolution of the  $2 \rightarrow 2$  subprocess  $u\bar{u} \rightarrow \gamma\gamma$  amplitude with the two splitting functions  $I_g^u(z)$  and  $I_u^g(z)$  which define in the collinear approximation the initial state radiative corrections. The final

state radiative corrections are denoted by  $F_j^i(z)$  (for the partonic specie  $j$  radiated from  $i$  with the momentum fraction  $z$  calculated as the leading log splitting function). While the agreement of total rates with such approximations is usually rather good, large deviations of distributions and event orientation may take place. For example, jets are effectively generated from the gluon radiation in the initial state of the  $2 \rightarrow 2$  subprocess  $q\bar{q} \rightarrow \gamma\gamma$  (see the first term in  $A_{34}$ ), while in CompHEP they evolve from two partons which are in the final state of various  $2 \rightarrow 4$  channels, see Table 1. Much enhanced jet activity in the central region is natural to expect with various diagrams of  $s$ -channel topologies (see e.g. diagrams 9,11,13 in Fig.1). Diagrams beyond the  $t$ -channel quark exchange  $q\bar{q} \rightarrow \gamma\gamma$  lead to broader rapidity distributions  $\Delta y_{\gamma\gamma}$  and  $\Delta y_{jet,jet}$ , the latter is especially important in view of the procedure for Higgs signal separation.

The only essential procedure beyond the automatic computation regime of CompHEP that must be performed by the user and which critically reduces the computation time and improves the quality of results is the procedure of phase space parametrization with the following replacements of phase space variables, which remove numerous "peaks" of the squared amplitude. Efficient Monte Carlo (MC) integration in the presence of multiple "peaks" associated with radiation of photons and gluons leading to the well-known collinear and infrared poles is very untrivial. Singularities also appear in the case when photons or gluons split into light quark-antiquark pairs or gluon splits into a pair of gluons. Such "fine tuning of the numerical interface" oftenly causes questions, so as a useful example we show in Fig.2 a set of phase space regularizations for the subprocess  $u\#g \rightarrow \gamma\gamma gu\#$ , see diagrams in Fig.1.

Momentum	> Mass	< > Width	<  Power
13	0	0	1
14	0	0	1
15	0	0	1
25	0	0	1
26	0	0	1
134	0	0	2
135	0	0	2
145	0	0	2
236	0	0	2
256	0	0	2
246	0	0	2
36	0	0	1
46	0	0	1
56	0	0	1
356	0	0	2
456	0	0	2
346	0	0	2
12	0	0	2

**Figure 2:** The set of 18 phase space mappings (kinematical regularizations) in CompHEP format for the main subprocess  $u\#g \rightarrow \gamma\gamma gu\#$ , see diagrams in Fig.1 and cross sections in Table 1. Numbers in the process string are assigned as  $12 \rightarrow 3456$ . Default  $t$ -channel kinematical scheme  $12 \rightarrow 3, 456, 456 \rightarrow 4, 56$  is used. With a reasonable number of MC sample points of the order of  $10^5$  for the one MC iteration, the accuracy of the cross section calculation with these mappings introduced reaches 0.2-0.3 % (at the  $1\sigma$  level) with ten iterations. The efficiency of unweighted event generation exceeds  $10^{-3}$ .

The first regularization labeled '13' in the left column in Fig.2 removes the first-order  $1/t$  pole for the transferred momentum  $t_{13} = (p_1 - p_3)^2$ , see diagrams 1-8, where  $p_1$  is the  $u\#$ -quark

momentum (first particle in the process string) and  $p_3$  is the photon momentum (third particle in the list). Analogously, the second regularization labeled '14' in the left column, removes the pole of the second photon (particle number 4 in the process string). The lines '15' and '25' are introduced to regularize the poles of diagrams 10, 12 and 14. The sixth regularization labeled 134 regularizes the second-order pole  $t_{134} = (p_1 - p_3 - p_4)$  in the central part of the ladder diagrams 2 and 3, which is not cancelled to the first-order pole, as it happens with  $t_{13, \dots, t_{26}}$  due to  $U(1)_{em}$  gauge invariance of the amplitude. The regularization '356' is introduced to remove the  $s$ -channel quark poles in diagrams 4, 6, 9 and 11, which appear when  $s_{356} = (p_3 + p_5 + p_6)^2$  is very small. The second-order peaks associated with vector bosons occur in the electroweak background diagrams. More examples of phase-space mappings can be found in [23]. High quality of unweighted events can be achieved, see some examples of distributions in Fig.3.

An information about colorless pairs (so-called color chains), needed to be transferred to PYTHIA package for simulation of jet fragmentation and hadronization, is obtained by decomposition of the color structures of diagrams  $C_{col}$  for a given partonic subprocess over the color basis in the limit  $N_c \rightarrow \infty$ :  $M_{col} = \sum C_{col}^i t_i$ , where  $t_i t_j = \delta_{ij}$ . For each unweighted event a set of color chains is generated. Events of various subprocesses are mixed randomly in one event flow taking into account their relative weights  $\sigma_i / \sum \sigma_i$ , where  $\sigma_i$  is the cross section of the  $i$ -th subprocess, see Table 1.

Most recent CompHEP version 4.5 (2009) provides the user with scripts to carry out noninteractive calculations in both symbolic and numerical modes on farms with parallel processors. PBS and LSF batch calculation shells are supported. The first unified format for unweighted events, LHA (Les Houches Accord) [18], which is used for transferring events from automatic calculation systems to the programs for showering and hadronisation, PYTHIA and HERWIG, and the following extensions, LHAPDF (for standardization of partonic distribution functions) [19], SUSY LHA (format for supersymmetric extensions of the SM, e.g. SUGRA and GMSB) [20], and LHE (universal format for unweighted events with HEPML descriptions) [21], have been implemented in CompHEP output. Support of the BSM LHA format [22] is in progress. Generation of ROOT-format source files have been developed for efficient construction of particle distributions. Monte Carlo event database (MCDB of CMS) has been developed as the universal shell for storing the unweighted events produced by different generators in the abovementioned universal formats.

Important development related not only to CompHEP but to all event generators which are able to produce an output in the universal format is a central Monte Carlo events database (MCDB) of CERN. It follows from the existing experience that the correct MC simulation of complicated multiparticle exclusive channels requires a rather sophisticated expertise. Rather often different experimental collaborations request an information from authors of MC generators relevant to the case of the same unweighted event samples, so various event samples stored in a public database could help to prevent losses of human and computing resources. A proposal for LCG MCDB project was presented in 2003 at the Les Houches workshop. More details can be found at <http://mcdb.cern.ch>

	subprocess	$\sigma$ , [pb]	$\frac{\sigma}{\sigma_{max}}$		subprocess	$\sigma$ , [pb]	$\frac{\sigma}{\sigma_{max}}$
1	$u\#, u\# \rightarrow A, A, u\#, u\#$	2.33	0.18		$u\#, u\# \rightarrow A, G, u\#, u\#$	514.1	0.36
2	$u\#, U\# \rightarrow A, A, u\#, U\#$	1.63	0.13		$u\#, U\# \rightarrow A, G, u\#, U\#$	123.2	0.09
3	$u\#, U\# \rightarrow A, A, d\#, D\#$	0.08	0.01		$u\#, U\# \rightarrow A, G, d\#, D\#$	0.3	0.00
4	$u\#, U\# \rightarrow A, A, G, G$	0.70	0.05		$u\#, U\# \rightarrow A, G, G, G$	2.4	0.00
5	$u\#, d\# \rightarrow A, A, u\#, d\#$	1.03	0.08		$u\#, d\# \rightarrow A, G, u\#, d\#$	208.1	0.15
6	$u\#, D\# \rightarrow A, A, u\#, D\#$	0.48	0.04		$u\#, D\# \rightarrow A, G, u\#, D\#$	101.4	0.07
7	$u\#, G \rightarrow A, A, G, u\#$	12.59	1.00		$u\#, G \rightarrow A, u\#, u\#, U\#$	52.5	0.04
8	$U\#, u\# \rightarrow A, A, u\#, U\#$	1.64	0.13		$U\#, G \rightarrow A, u\#, d\#, D\#$	30.3	0.02
9	$u\#, U\# \rightarrow A, A, d\#, D\#$	0.08	0.01		$u\#, G \rightarrow A, G, G, u\#$	1397.7	1
10	$U\#, u\# \rightarrow A, A, G, G$	0.70	0.06		$U\#, u\# \rightarrow A, G, u\#, U\#$	125.7	0.09
11	$U\#, U\# \rightarrow A, A, U\#, U\#$	0.23	0.02		$U\#, u\# \rightarrow A, G, d\#, D\#$	0.3	0.00
12	$U\#, d\# \rightarrow A, A, U\#, d\#$	0.26	0.02		$U\#, u\# \rightarrow A, G, G, G$	2.4	0.00
13	$U\#, D\# \rightarrow A, A, U\#, D\#$	0.19	0.02		$U\#, U\# \rightarrow A, G, U\#, U\#$	19.1	0.01
14	$U\#, G \rightarrow A, A, G, U\#$	2.94	0.23		$U\#, d\# \rightarrow A, G, U\#, d\#$	41.9	0.03
15	$d\#, u\# \rightarrow A, A, u\#, d\#$	1.02	0.08		$U\#, D\# \rightarrow A, G, U\#, D\#$	17.2	0.01
16	$d\#, U\# \rightarrow A, A, U\#, d\#$	0.26	0.02		$U\#, G \rightarrow A, u\#, U\#, U\#$	8.5	0.01
17	$u\#, d\# \rightarrow A, A, u\#, d\#$	0.08	0.01		$U\#, G \rightarrow A, U\#, d\#, D\#$	4.5	0.00
18	$d\#, D\# \rightarrow A, A, u\#, U\#$	0.03	0.00		$U\#, G \rightarrow A, G, G, U\#$	196.5	0.14
19	$d\#, D\# \rightarrow A, A, d\#, D\#$	0.08	0.01		$d\#, u\# \rightarrow A, G, u\#, d\#$	206.9	0.15
20	$d\#, D\# \rightarrow A, A, G, G$	0.03	0.00		$d\#, U\# \rightarrow A, G, U\#, d\#$	41.9	0.03
21	$d\#, G \rightarrow A, A, G, d\#$	0.49	0.04		$d\#, d\# \rightarrow A, G, d, d\#$	49.7	0.03
22	$D\#, u\# \rightarrow A, A, u\#, D\#$	0.48	0.04		$d\#, D\# \rightarrow A, G, u\#, U\#$	0.1	0.00
23	$D\#, U\# \rightarrow A, A, u\#, D\#$	0.19	0.02		$d\#, D\# \rightarrow A, G, d\#, D\#$	23.3	0.02
24	$D\#, d\# \rightarrow A, A, u\#, U\#$	0.03	0.00		$d\#, D\# \rightarrow A, G, G, G$	0.4	0.00
25	$D\#, d\# \rightarrow A, A, d\#, D\#$	0.08	0.01		$d\#, G \rightarrow A, u\#, U\#, d\#$	23.9	0.02
26	$D\#, d\# \rightarrow A, A, G, G$	0.03	0.00		$d\#, G \rightarrow A, d\#, d\#, D\#$	8.0	0.00
27	$D\#, D\# \rightarrow A, A, D\#, D\#$	0.02	0.00		$d\#, G \rightarrow A, G, G, d\#$	195.2	0.14
28	$D\#, G \rightarrow A, A, G, D\#$	0.23	0.02		$D\#, u\# \rightarrow A, G, u\#, D\#$	98.7	0.07
29	$G, u\# \rightarrow A, A, G, u\#$	12.60	1.00		$D\#, U\# \rightarrow A, G, U\#, D\#$	17.6	0.01
30	$G, U\# \rightarrow A, A, G, U\#$	2.92	0.23		$D\#, d\# \rightarrow A, G, u\#, U\#$	0.1	0.00
31	$G, d\# \rightarrow A, A, G, d\#$	0.49	0.04		$D\#, d\# \rightarrow A, G, d\#, D\#$	23.2	0.02
32	$G, D\# \rightarrow A, A, G, D\#$	0.24	0.02		$D\#, d\# \rightarrow A, G, G, G$	0.4	0.00
33	$G, G \rightarrow A, A, u\#, U\#$	2.81	0.22		$D\#, D\# \rightarrow A, G, D\#, D\#$	9.0	0.00
34	$G, G \rightarrow A, A, d\#, D\#$	0.18	0.01		$D\#, G \rightarrow A, u\#, U\#, D\#$	9.6	0.00
35					$D\#, G \rightarrow A, d\#, D\#, D\#$	2.8	0.00
36					$D\#, G \rightarrow A, G, G, D\#$	69.1	0.05
37					$G, u\# \rightarrow A, u\#, u\#, U\#$	53.3	0.04
38					$G, u\# \rightarrow A, u\#, d\#, D\#$	29.7	0.02
39					$G, u\# \rightarrow A, G, G, u\#$	1400.0	1
40					$G, U\# \rightarrow A, u\#, U\#, U\#$	9.5	0.00
41					$G, U\# \rightarrow A, U\#, d\#, D\#$	4.5	0.00
42					$G, U\# \rightarrow A, G, G, U\#$	198.6	0.14
43					$G, d\# \rightarrow A, u\#, U\#, d\#$	23.8	0.02
44					$G, d\# \rightarrow A, d\#, d\#, D\#$	7.7	0.00
45					$G, d\# \rightarrow A, G, G, d\#$	190.9	0.13
46					$G, D\# \rightarrow A, u\#, U\#, D\#$	9.9	0.00
47					$G, D\# \rightarrow A, G, G, D\#$	2.9	0.00
48					$G, D\# \rightarrow A, G, G, D\#$	68.8	0.05
49					$G, G \rightarrow A, G, u\#, U\#$	277.9	0.20
50					$G, G \rightarrow A, G, d\#, D\#$	69.5	0.05
all	$pp \rightarrow A, A, j, j$	47.24			$pp \rightarrow A, j, j, j$	5970.4	

**Table 1:** Cross sections of individual partonic subprocesses contributing to irreducible (left column) and misidentification (right column) backgrounds  $pp \rightarrow \gamma\gamma+2$  jets and  $pp \rightarrow \gamma+3$  jets. CompHEP notation  $u\#$  and  $d\#$  for up and down quarks ( $U\#$  and  $D\#$  for antiquarks) is introduced to calculate conveniently Feynman diagrams with numerous possible combinations of initial and final quarks with different flavors (see [17] for details). The parameter values  $\alpha_e = 1/137$  (i.e.  $e = 0.3029$ ) and  $\alpha_s = 0.1298$  ( $g_s = \sqrt{4\pi\alpha_s} = 1.2772$ ). PDF set CTEQ5L [16], PDF factorization scale 50 GeV.

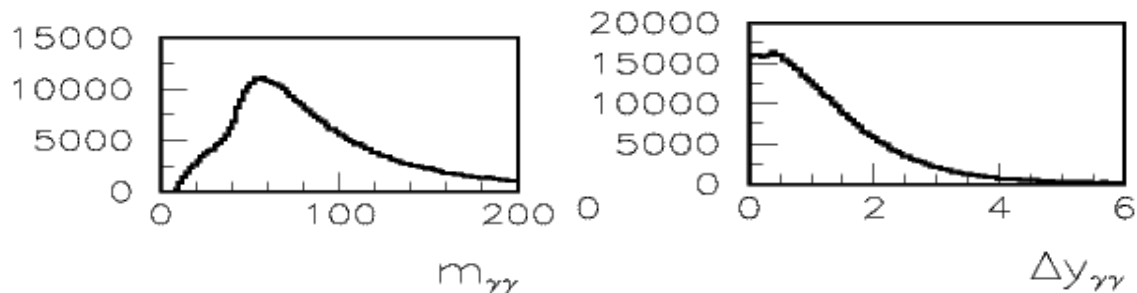


**Figure 3:** Partonic level distributions  $d\sigma/dM_{\gamma\gamma}$  and  $d\sigma/dy_{\gamma\gamma}$  for the process  $pp \rightarrow \gamma\gamma + 2$  jets generated using 500K QCD unweighted event sample.

### 3. Summary

The ideology of automatic generation of amplitudes and the precise Monte Carlo calculation of complete tree-level diagram sets with the subsequent generation of unweighted events demonstrated over the last two decades its efficiency for direct simulation of processes in Tevatron and LHC detectors.

Main directions of CompHEP development in the recent years have been (1) porting the computation of numerous partonic subprocesses and the generation of unweighted events to multi-processor farms, important in particular for LHC simulations, where the number of subprocesses that must be accounted for amounts to several hundred, (2) creation of interfaces to the programs for parton showering and hadronization and for detector simulation packages, (3) development of universal formats for output event files.

The number of studies which are using various extensions of the Standard Model in CompHEP format, published by users of the package, is impressively large. However one should note that beyond the "proliferation" of chiral  $SU(2)$  multiplets and singlets of fundamental fermions, CompHEP version 4 provides rather restricted possibilities for work with models of higher-rank gauge symmetry groups. Rich possibilities are going to be implemented in version 5 of CompHEP, which includes the symbolic calculation kernel based on FORM [24].

Note that fully automatic software packages for calculations at the one-loop level or at the NLO level of accuracy do not exist at present time, although intense work is being performed to create them. Although CompHEP is a tree-level package, in a number of cases next-to-leading order (NLO) corrections can be included. At the tree-level  $N$ -particle final state the NLO correction  $pp \rightarrow N+1$  to the  $pp \rightarrow N$  can be always calculated. NLO structure functions,  $K$ -factors and other local effective factors from multiloop diagrams can be taken into account. However in each particular case correct matching of tree-level to NLO result should be carefully analyzed with an appropriate choice of the corresponding energy/momentum separation or factorization scales.

*Acknowledgements.* Work was partially supported by grants ADTP 3341, RFBR 10-02-00525-a, NS 1456.2008.2 and FAP contract 5163.



## References

- [1] E.E. Boos, M.N. Dubinin, V.F. Edneral, V.A. Ilyin, A.P. Kryukov, A.E. Pukhov, A.Ya. Rodionov, V.I. Savrin, D.A. Slavnov, A.Yu. Taranov, *CompHEP - computer system for calculation of particle collisions at high energies*, SINP MSU report 89-63/140, 1989
- [2] A.C.Hearn, *REDUCE user's manual*, version 3.5, RAND publication 1993
- [3] E.E. Boos, M.N. Dubinin, V.F. Edneral, V.A. Ilyin, A.P. Kryukov, A.E. Pukhov, S.A. Shichanin, *Applications of CompHEP system to particle processes calculation*, SINP MSU report 91-9/213, 1991
- [4] S.Kawabata, *A New Monte Carlo Event Generator for High-Energy Physics*, *Comp.Phys.Commun.* **41**, 127 (1986)  
S.Kawabata, in: *New Computing Techniques in Physics Research, Proc. of 2nd International Workshop on Software Engineering, Artificial Intelligence and Expert Systems for High-energy and Nuclear Physics*, La Londe Les Maures, France, 13-18 January 1992, p. 745
- [5] T.Ishikawa, T.Kaneko, K.Kato, S.Kawabata, Y.Shimizu, H.Tanaka, *GRACE manual: Automatic generation of tree amplitudes in Standard Models: Version 1.0*, KEK report 92-19, 1993
- [6] E.Boos, M.Dubinin, V.Edneral, V.Ilyin, A.Pukhov, S.Shichanin, T.Kaneko, S.Kawabata, Y.Kurihara, Y.Shimizu, H.Tanaka, *Automatic calculation in high-energy physics by Grace/Chanel and CompHEP*, *Int.J.Mod.Phys.*, **C5**, 615 (1994)
- [7] E.E.Boos, M.N.Dubinin, V.A.Ilyin, A.E.Pukhov, in:  *$e^+e^-$  Collisions at 500 GeV: the Physics Potential*. Proc. of the Workshop Munich, Annecy, Hamburg, ed. by P.Zerwas, DESY report 93-123C, 1993, p.561
- [8] D.Bardin, R.Kleiss et al., in: *Physics at LEP2*, ed. by G.Altarelli, T.Sjostrand, F.Zwirner, CERN report 96-01, vol. I, Geneva, 1996, p. 3 (hep-ph/9709270)  
F.Boudjema, B.Mele et al., in: *Physics at LEP2*, ed. by G.Altarelli, T.Sjostrand, F.Zwirner, CERN report 96-01, vol. I, Geneva, 1996, p. 207 (hep-ph/9601224)  
Martin W. Grunewald, Giampiero Passarino et al., in: *Reports of the Working Groups on Precision Calculations for LEP2 Physics*, CERN report 009-A, Geneva, 2000, p. 1 (hep-ph/0005309)
- [9] E. Boos, V. Bunichev, M. Dubinin, L. Dudko, V. Edneral, V. Ilyin, A. Kryukov, V. Savrin, A. Semenov, A. Sherstnev, *CompHEP 4.5 Status Report*, arXiv:0901.4757 [hep-ph]  
E. Boos, V. Bunichev, M. Dubinin, L. Dudko, V. Ilyin, A. Kryukov, V. Edneral, V. Savrin, A. Semenov, A. Sherstnev, *CompHEP 4.4: Automatic computations from Lagrangians to events*, *Nucl. Instrum. Meth.* **A534**, 250 (2004) (hep-ph/0403113)  
A.Pukhov et al, *CompHEP - a package for evaluation of Feynman diagrams and integration over multi-particle phase space*. User's manual for version 3.3, INP MSU report 98-41/542 (hep-ph/9908288)  
see also <http://theory.sinp.msu.ru/comphep>
- [10] E.E. Boos, V.E. Bunichev, L.V. Dudko, V.I. Savrin and A.V. Sherstnev, *Method for simulating electroweak top-quark production events in the NLO approximation: SingleTop event generator*, *Phys. Atom. Nucl.* **69**, 1317 (2006) (*Yad. Fiz.* **69**, 1352 (2006))  
V.M. Abazov et al. [D0 Collaboration], *Evidence for production of single top quarks*, *Phys. Rev.* **D78**, 012005 (2008) (arXiv:0803.0739 [hep-ex])

- [11] C. Seez and J. Virdee, *Detection of an intermediate mass Higgs boson at LHC via its two photon decay mode*, CMS TN/92-56, 1992  
CMS Collaboration, *The Electromagnetic Calorimeter Project - Technical Design Report*, CERN/LHCC 97-33, 1997
- [12] M. Dubinin, V. Litvin, Y. Ma, H. Newman, M. Pieri, *The vector boson fusion production with  $H \rightarrow \gamma\gamma$* , CMS Analysis Note 2006/097, 2006
- [13] D. Rainwater and D. Zeppenfeld, *Searching for  $H \rightarrow \gamma\gamma$  in weak boson fusion at the LHC*, JHEP **12**, 5 (1997)
- [14] M.N. Dubinin, *Higgs Boson Signal in the Reaction  $pp \rightarrow \gamma\gamma + 2$  forward jets*, CMS Note 2001/022, 2001  
M.N. Dubinin, V.A. Ilyin, V.I. Savrin, *Light Higgs Boson Signal at LHC in the Reactions  $pp \rightarrow \gamma\gamma + jet$  and  $pp \rightarrow \gamma\gamma + lepton$* , CMS Note 1997/101, 1997
- [15] T. Sjöstrand, *Comput. Phys. Commun.* **82**, 74 (1994)  
T. Sjöstrand et al., *Comput. Phys. Commun.* **135**, 238 (2001) (hep-ph/0010017)
- [16] CTEQ Collaboration, H.L. Lai et al., *Global QCD Analysis of Parton Structure of the Nucleon: CTEQ5 Parton Distributions*, *Eur. Phys. J.* **C12**, 375 (2000)
- [17] E.E. Boos, V.A. Ilyin and A.N. Skachkova, *Simplification of flavor combinatorics in evaluation of hadronic processes*, JHEP **0005**, 052 (2000) (hep-ph/0004194)
- [18] E. Boos et al., *Generic user process interface for event generators*, hep-ph/0109068
- [19] M.R. Whalley, D. Bourilkov and R.C. Group, *The Les Houches accord PDFs (LHAPDF) and LHAGLUE*, hep-ph/0508110
- [20] P. Skands et al., *SUSY Les Houches accord: Interfacing SUSY spectrum calculators, decay packages, and event generators*, JHEP **0407**, 036 (2004) (hep-ph/0311123)
- [21] J. Alwall et al., *A Standard format for Les Houches event files*, *Comp. Phys. Commun.*, **176**, 300 (2007) (hep-ph/0609017)
- [22] J. Alwall et al., *A Les Houches Interface for BSM Generators*, arXiv:0712.3311[hep-ph]
- [23] E.E. Boos, M.N. Dubinin, *Problems of Automatic Calculation for Collider Physics*, *Uspekhi Fiz. Nauk*, **180**, 1081 (2010)
- [24] J.A.M. Vermaseren, *Symbolic Manipulation with FORM* (Amsterdam, Computer Algebra Netherlands, 1991)